

General Disclaimer

One or more of the Following Statements may affect this Document

- This document has been reproduced from the best copy furnished by the organizational source. It is being released in the interest of making available as much information as possible.
- This document may contain data, which exceeds the sheet parameters. It was furnished in this condition by the organizational source and is the best copy available.
- This document may contain tone-on-tone or color graphs, charts and/or pictures, which have been reproduced in black and white.
- This document is paginated as submitted by the original source.
- Portions of this document are not fully legible due to the historical nature of some of the material. However, it is the best reproduction available from the original submission.

**NASA TECHNICAL
MEMORANDUM**

NASA TM X-74010

NASA TM X-74010

(NASA-TM-X-74010) LOW-SPEED POWER EFFECTS
ON ADVANCED FIGHTER CONFIGURATIONS WITH
TWO-DIMENSIONAL DEFLECTED THRUST (NASA)
21 p HC A02/MF A01

N77-20077

CSSL 01C

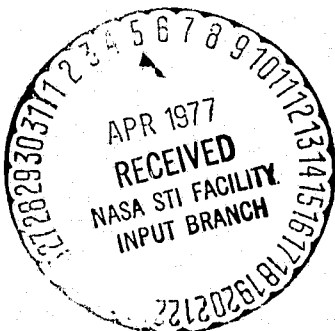
G3/05

Unclas
21711

**LOW-SPEED POWER EFFECTS ON ADVANCED FIGHTER CONFIGURATIONS
WITH TWO-DIMENSIONAL DEFLECTED THRUST**

John W. Paulson, Jr.; James L. Thomas; and Long P. Yip

This informal documentation medium is used to provide accelerated or special release of technical information to selected users. The contents may not meet NASA formal editing and publication standards, may be revised, or may be incorporated in another publication.



NASA
National Aeronautics and
Space Administration
Langley Research Center
Hampton, Virginia 23665

February 1977

1. Report No. NASA TM X-74010		2. Government Accession No.		3. Recipient's Catalog No.	
4. Title and Subtitle LOW-SPEED POWER EFFECTS ON ADVANCED FIGHTER CONFIGURATIONS WITH TWO-DIMENSIONAL DEFLECTED THRUST				5. Report Date February 1977	
				6. Performing Organization Code	
7. Author(s) John W. Paulson, Jr.; James L. Thomas; and Long P. Yip				8. Performing Organization Report No.	
				10. Work Unit No. 505-11-24-02	
9. Performing Organization Name and Address NASA Langley Research Center Hampton, Va. 23665				11. Contract or Grant No.	
				13. Type of Report and Period Covered Technical Memorandum	
12. Sponsoring Agency Name and Address National Aeronautics and Space Administration Washington, D.C. 20546				14. Sponsoring Agency Code	
15. Supplementary Notes					
16. Abstract <p>Wind-tunnel studies at the Langley Research Center have shown that significant increases in maximum lift coefficient and stability and decreases in drag due to lift are obtained when two-dimensional vectored thrust is used in conjunction with a close-coupled canard. The configuration tested was somewhat above the theoretical minimum drag due to lift because of the sharp leading edge on the biconvex airfoil used on the wing and canard. An effort to design a new configuration which will approach the minimum drag due to lift while maintaining high-lift configurations has been completed. The resulting model will incorporate a realistic planform, airfoil section, and twist for a transonic maneuvering configuration.</p>					
17. Key Words (Suggested by Author(s))			18. Distribution Statement Unclassified - Unlimited		
			Subject Category		
19. Security Classif. (of this report) Unclassified		20. Security Classif. (of this page) Unclassified		21. No. of Pages 18	22. Price* \$3.50

LOW-SPEED POWER EFFECTS ON ADVANCED FIGHTER CONFIGURATIONS
WITH TWO-DIMENSIONAL DEFLECTED THRUST

John W. Paulson, Jr.; James L. Thomas; and
Long P. Yip

Langley Research Center

SUMMARY

Wind-tunnel studies at the Langley Research Center have shown that significant increases in maximum lift coefficient and stability and decreases in drag due to lift are obtained when two-dimensional vectored thrust is used in conjunction with a close-coupled canard. The configuration tested was somewhat above the theoretical minimum drag due to lift because of the sharp leading edge on the biconvex airfoil used on the wing and canard. An effort to design a new configuration which will approach the minimum drag due to lift while maintaining high-lift coefficients has been completed. The resulting model will incorporate a realistic planform, airfoil section, and twist for a transonic maneuvering configuration.

INTRODUCTION

Extensive unpowered studies by Blair B. Gloss at the Langley Research Center (refs. 1 to 5) have shown the increases in maximum lift coefficient that are obtained with close-coupled canard/strake fighter configurations. Analysis of the data of reference 2 shows a reduction in drag due to lift due to both the canard/strake and wing camber. (See refs. 6 and 7.) These benefits, however, are accompanied at the higher lift coefficients by rather high longitudinal instabilities, or pitchup, due to the vortex lift from the strakes.

Recent experimental studies of a powered scaled-up version of Gloss' uncambered configuration in the Langley V/STOL tunnel have shown a significant reduction in the pitchup, along with further reductions in drag due to lift, due to power.

The model tested in the Langley V/STOL tunnel had little or no design optimization in that the wing and canard had no twist, camber, or leading-edge radius. Therefore, if proper attention were given to planform geometry, twist, camber, and airfoil section, it would seem that further reductions in drag due to lift should be possible. The favorable power effects should maintain the stability levels that were obtained in the powered tests discussed here. A new aerodynamic design study has been completed with the resulting model being designed to meet maneuvering requirements at transonic speeds as well as high-lift requirements at low speeds.

This paper will address the theoretical and experimental studies of the basic close-coupled wing/canard/strake configuration and the aerodynamic design of the new transonic fighter configuration. Also, examples of some supersonic fighter configurations which are being considered for future aerodynamic design studies are discussed.

SYMBOLS

A	aspect ratio, $\frac{b^2}{S}$
b	span of wing or canard (with subscript), m (ft)
C_D	drag coefficient, $\frac{\text{Drag}}{q_\infty S}$
C_{D_i}	drag coefficient due to lift, $C_{D_i} = C_D - C_{D_0}$
C_{D_0}	zero lift drag coefficient

C_L	lift coefficient, $\frac{\text{Lift}}{q_\infty S}$
C_l	section-lift coefficient, $\frac{\text{Lift}}{q_\infty c}$
C_m	pitching-moment coefficient, $\frac{\text{Pitching moment}}{q_\infty S \bar{c}}$
C_p	pressure coefficient, $\frac{\text{Pressure}}{q_\infty S}$
C_T	thrust coefficient, $\frac{\text{Static thrust}}{q_\infty S}$
$\frac{C_D - C_{D_0} - C_T \sin(\alpha + \delta)}{[C_L - C_T \cos(\alpha + \delta)]^2}$	drag due to lift parameter, $\frac{1}{\pi A_e}$
c	chord, m (ft)
\bar{c}	mean aerodynamic chord, m (ft)
e	drag due to lift efficiency factor, $\frac{C_{Di}}{C_L^2} \pi A$
M	Mach number
q_∞	free-stream dynamic pressure, Pa (psf)
S	wing area, m^2 (ft^2)
t	airfoil-section thickness, m (ft)
x, y, z	orthogonal coordinate system from model nose, m (ft)
α	angle of attack, deg
δ	deflection angle, deg

ϵ	twist, deg
η	nondimensional semispan, $\frac{y}{b/2}$
Λ	sweep angle, deg
Subscripts:	
c	canard
c.p.	center of pressure
D.D.	drag divergence
f	flap
max	maximum
N	nozzle
∞	free stream
\perp	perpendicular

DISCUSSION

Theoretical studies of the configuration shown in figures 1 and 2 were compared with the data of reference 2. This comparison is shown in figure 3. The agreement between theory (ref. 8) and experiment is seen to be quite good over the linear range of the data. The theory does not predict the vortex lift and resulting pitching moment when the strakes are added to the configuration. These studies allowed a prediction of the model moment center to give a longitudinal instability of 5 percent ($\partial C_m / \partial C_L = 0.05$) at low C_L for the V/STOL tunnel tests.

The model used in the V/STOL tunnel tests is shown in figures 1 and 2. The geometry of the model was identical to the unpowered model tests in the Langley 7- by 10-foot tunnel except for installation of two-dimensional nozzles at the wing root and different canard strakes. The longitudinal data for the configuration without strakes are shown in figure 4. The data show that at the lower C_L 's, power off, the configuration has a $\partial C_m / \partial C_L = 0.06$, about as predicted. The data also show that when the flaps are deflected 30° , power off, pitchup occurs ($\partial C_m / \partial C_L = 0.13$) even without the strake due to flow separation over the flaps. The pitchup was eliminated, $\partial C_m / \partial C_L = 0$, over a large C_L range with a $C_T = 0.3$. Figure 5 shows the longitudinal data for the configuration with strakes. At the lower C_L 's, power off, the configuration has a slight increase in instability ($\partial C_m / \partial C_L = 0.07$) due to the strake area being added forward on the model. At the higher C_L 's, there is more severe pitchup than was obtained without the strakes, especially for $\delta_f = 30^\circ$ where $\partial C_m / \partial C_L = 0.30$ at $\alpha = 20^\circ$ to 25° . This pitchup, prior to $C_{L_{max}}$, due to the strake vortex lift is significant and was also shown by Gloss. The effect of power was to reduce the pitch instability to $\partial C_m / \partial C_L = 0.11$ for $\alpha = 20^\circ$ to 25° .

Previous analyses of reference 2 data are presented in references 6 and 7 and show the reductions in drag due to lift when the canard and strake were added to the wing. The V/STOL tunnel data, shown in figure 6, show the same trends as before without power and show further reductions in drag due to lift with power. The term $\frac{C_D - C_{D_0} + C_T \cos(\alpha + \delta)}{[C_L - C_T \sin(\alpha + \delta)]^2}$ is an experimental thrust removed $\Delta C_D / C_L^2$ or $1/\pi A e$. The theoretical minimum was obtained by calculating the optimum C_{D_i} for the configuration. It can be seen that although further reductions in $\Delta C_D / C_L^2$ occurred due to power, none of the curves reached the theoretical minimum. This is because the wing and canard were uncambered with

a sharp leading edge. A configuration with appropriate twist, camber, and leading-edge radius should show the same trends as figure 6 and correlate better with the minimum value for $1/\pi A_e$ and should be able to be trimmed to C_{Lmax} .

A sketch of a new aerodynamic design for a transonic maneuvering configuration is shown in figure 7. This model will use the same fuselage and powered nozzles as the original configuration, shown as the dashed line in the figure. This planform was developed around the requirements that the two-dimensional nozzle location be the same as that for the original model and the wing sweep be increased to about 40° at $c/2$. The latter requirement was to give $M_{\perp} = 0.7$ at $M_{\infty} = 0.9$. The canard leading- and trailing-edge sweeps are the same as that for the wing. The canard taper ratio was picked so that a reasonable tip chord existed when the canard span was extended to equal the wing span. This was done to study the effect of canard to wing span ratio on drag due to lift. The canard thickness distribution, twist, and camber are shown in figures 8 and 9. A supercritical airfoil was modified for three-dimensional induced effects. Using the method of reference 9, a curve of C_{η} versus M_{DD} was developed for the airfoil. (See fig. 8.) At various spanwise stations on the wing and canard, the sweep of the (x/c) c.p. location was calculated, using the method of reference 8, to compute M_{\perp} . Using the M_{\perp} and the C_{η} versus M_{DD} curves, the C_{η} versus η curves of figure 8 were developed. These curves give the maximum free-stream C_{η} that the planform can have and stay below drag divergence. Figure 9 shows the input C_{η} versus η and chord loading for the design program. The C_{η} was chosen as an average of the maximum C_{η} from figure 8 and held constant across the span realizing that the root and tip area twists would have to be modified. The two-dimensional subcritical chord loading for the supercritical airfoil was used in a vortex-lattice program to define the

twist and camber shown in figure 9. The wing and canard angles of attack were 10° and the twists were fitted to the theoretical distributions as shown by the dashed line in the figure. This procedure was not intended to produce an optimum transonic design. Rather it was intended to develop a configuration with a wing and canard which would be representative of that required for transonic maneuvering to study high angle-of-attack aerodynamic and power effects. The configuration will employ full-span wing and canard flaps as well as leading-edge camber to provide high lift at low speeds. This configuration will be tested at low speeds in the V/STOL tunnel.

Follow-on designs that are being considered for a supersonic configuration are shown in figure 10. As in the transonic design, the intent will be to aerodynamically design the model to be representative of that needed for efficient supersonic cruise. However, it will be tested at low speeds in takeoff and landing and at high angles of attack. Two possible configurations are shown that may give good takeoff, landing, and maneuvering characteristics. One has an extensive leading-edge radius and variable camber in combination with a pop-out strake. The other has a variable glove section with leading-edge wing camber. Both concepts would use the vectored thrust as in the transonic design.

CONCLUDING REMARKS

The work of Gloss has shown the increases in $C_{L_{max}}$ and reduction in drag due to lift that are obtainable when a canard/strake is utilized with a fighter-type wing planform. Further increases in $C_{L_{max}}$ and reductions in drag due to lift have been demonstrated by the authors when power is employed in addition

to the canard/strake. Furthermore, the longitudinal instability, or pitchup, was significantly reduced with power.

An effort to aerodynamically design a more realistic planform, airfoil section, and twist for a maneuvering transonic configuration has been completed. The new configuration is under construction and will be tested at low speeds in the Langley V/STOL tunnel to study takeoff, landing, and high angle-of-attack aerodynamics with power.

REFERENCES

1. Gloss, Blair B.; and McKinney, Linwood W.: Canard-Wing Lift Interference Related to Maneuvering Aircraft at Subsonic Speeds. NASA TM X-2897, 1973
2. Gloss, Blair B.: The Effect of Canard Leading-Edge Sweep and Dihedral Angle on the Longitudinal and Lateral Aerodynamic Characteristics of a Close-Coupled Canard-Wing Configuration. NASA TN D-7214, 1976
3. Gloss, Blair B.: Effect of Wing Planform and Canard Location and Geometry on the Longitudinal Aerodynamic Characteristics of a Close-Coupled Canard-Wing Model at Subsonic Speeds. NASA TN D-7410, 1975
4. Miner, Dennis D.; and Gloss, Blair B.: Flow Visualization Study of Close-Coupled Canard-Wing and Strake-Wing Configuration. NASA TM X-72668, 1975
5. Gloss, Blair B.; Henderson, William P.; and Huffman, Jarrett K.: Effect of Canard Position and Wing Leading-Edge Flap Deflection on Wing Buffet at Transonic Speeds. NASA TM X-72681, 1975
6. Paulson, John W., Jr.: Applications of Vortex-Lattice Theory to Preliminary Aerodynamic Design. NASA SP-405, 1976, pp. 113-126
7. Tulinius, Jan R.; and Margason, Richard J.: Aircraft Aerodynamics Design and Evaluation Methods. AIAA Paper 76-15, 1976
8. Tulinius, J.: Unified Subsonic, Transonic, and Supersonic NAR Vortex Lattice. TFD-72-523, 1972, Rockwell International
9. Bauer, Frances; Garabedian, Paul; Korn, David; and Jameson, Antony: Supercritical Wing Sections II. Lecture Notes in Economics and Mathematical Systems, M. Beckman and H. P. Künzi, eds., Springer-Verlag, 1975

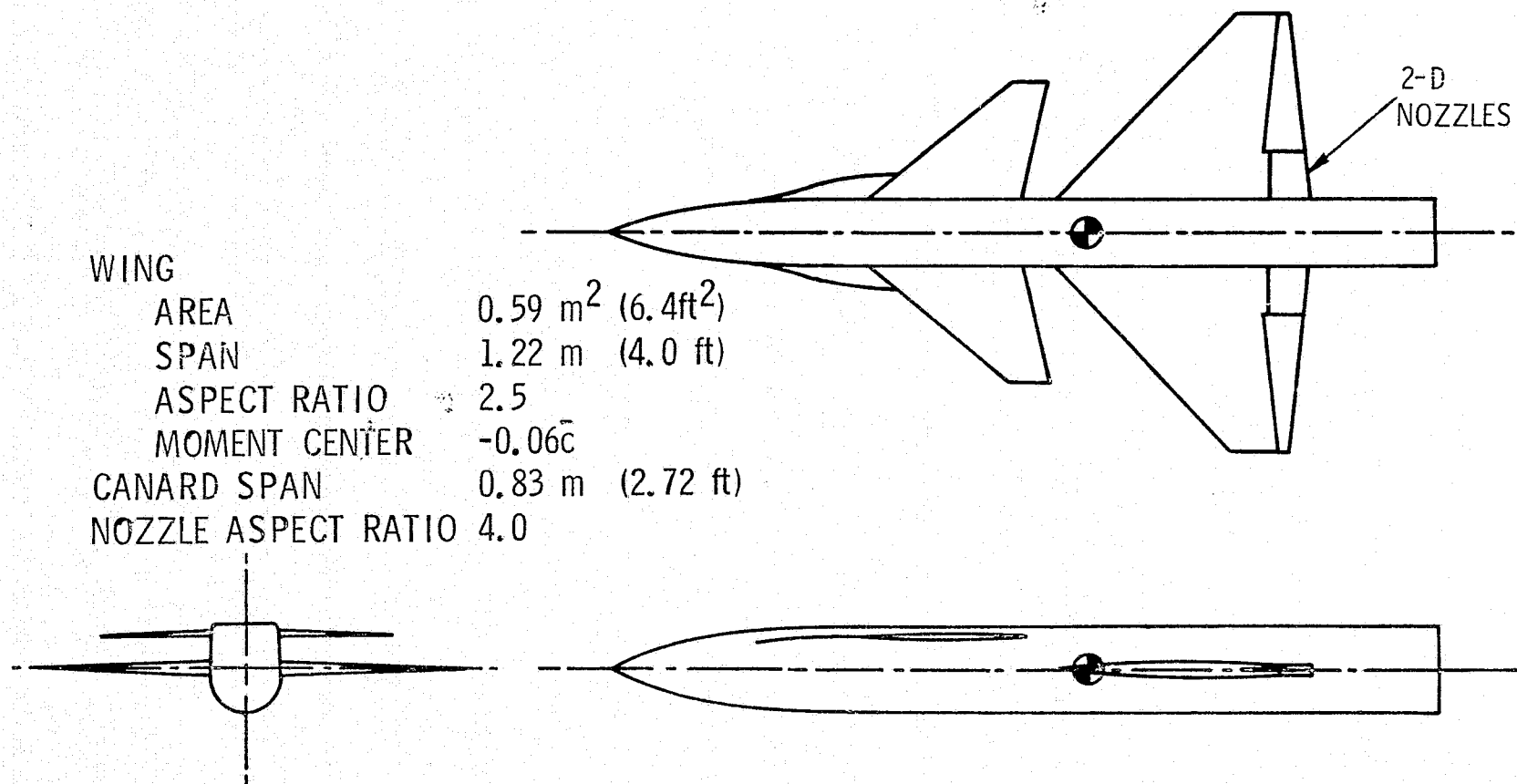


Figure 1. - Close-coupled wing-canard configuration.

ORIGINAL PAGE IS
OF POOR QUALITY

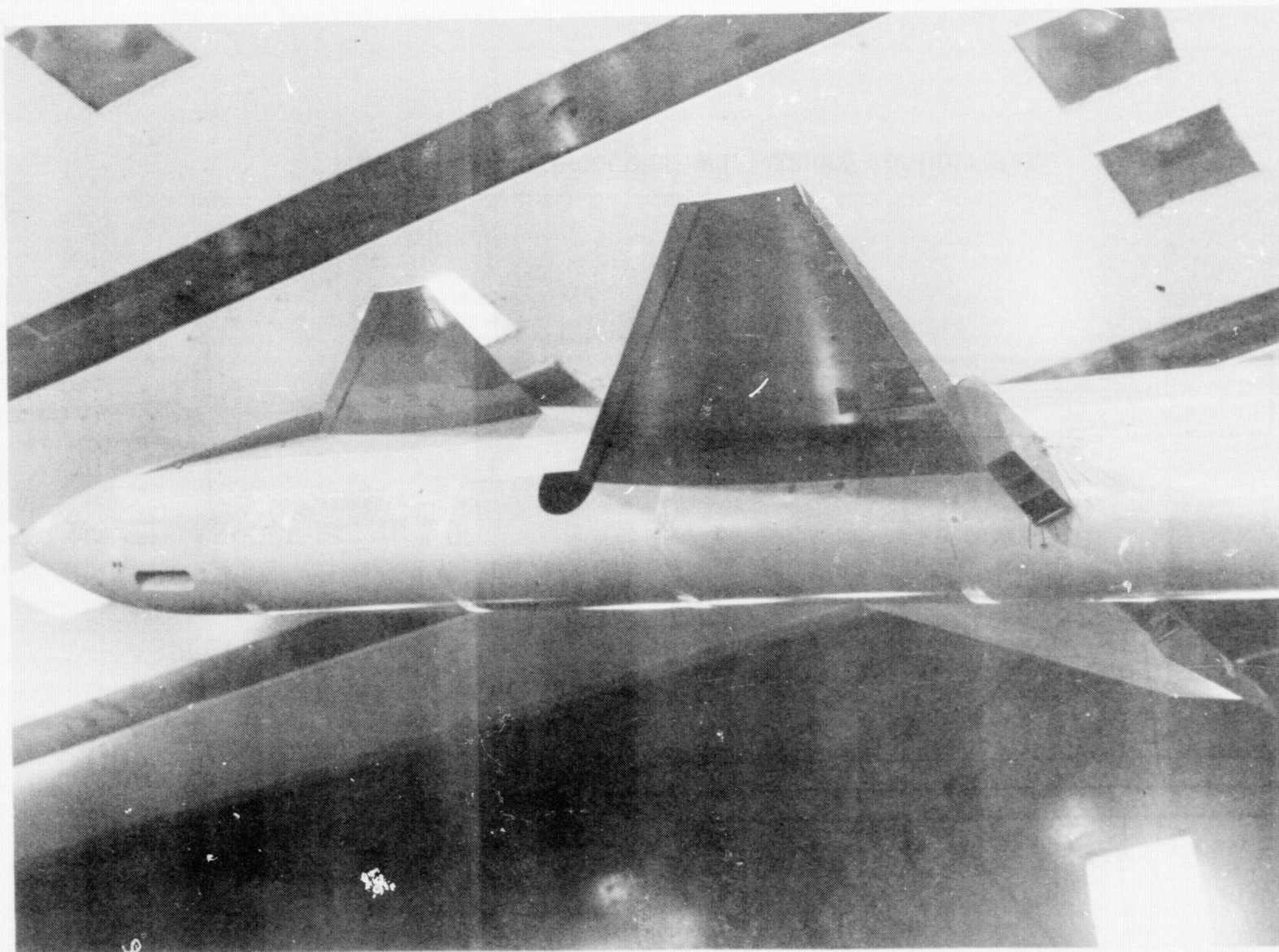


Figure 2. - Close-coupled wing-canard model installed in the V/STOL tunnel.

THEORY DATA
 VORTEX LATTICE GLOSS

——— ○ WING ALONE
 - - - □ WING CANARD

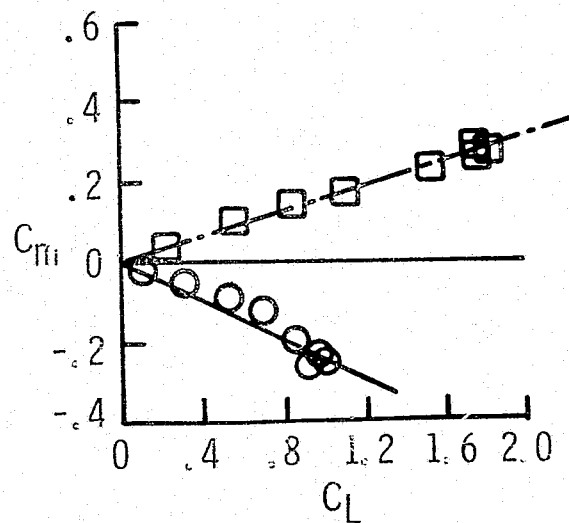
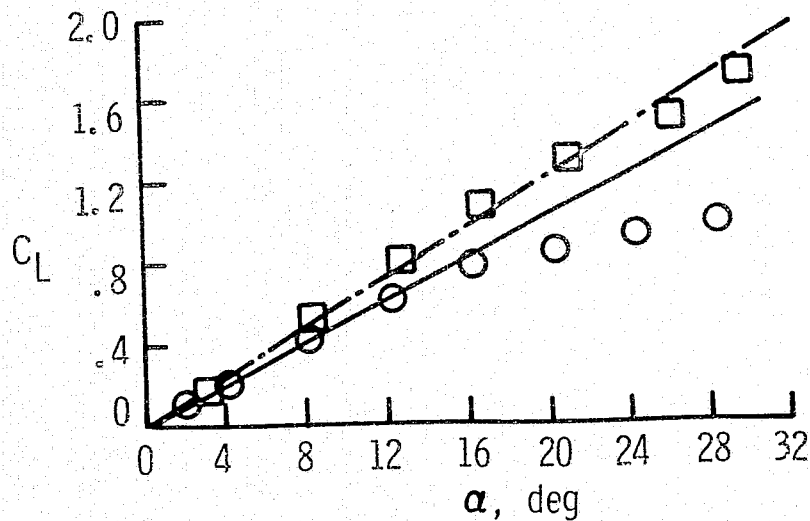
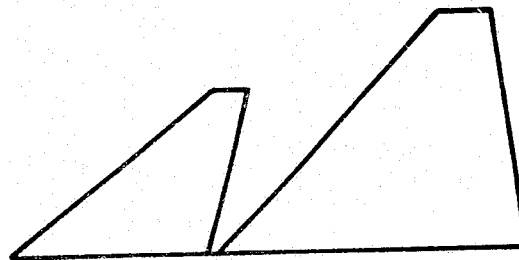


Figure 3. - Comparison between theory and experiment.

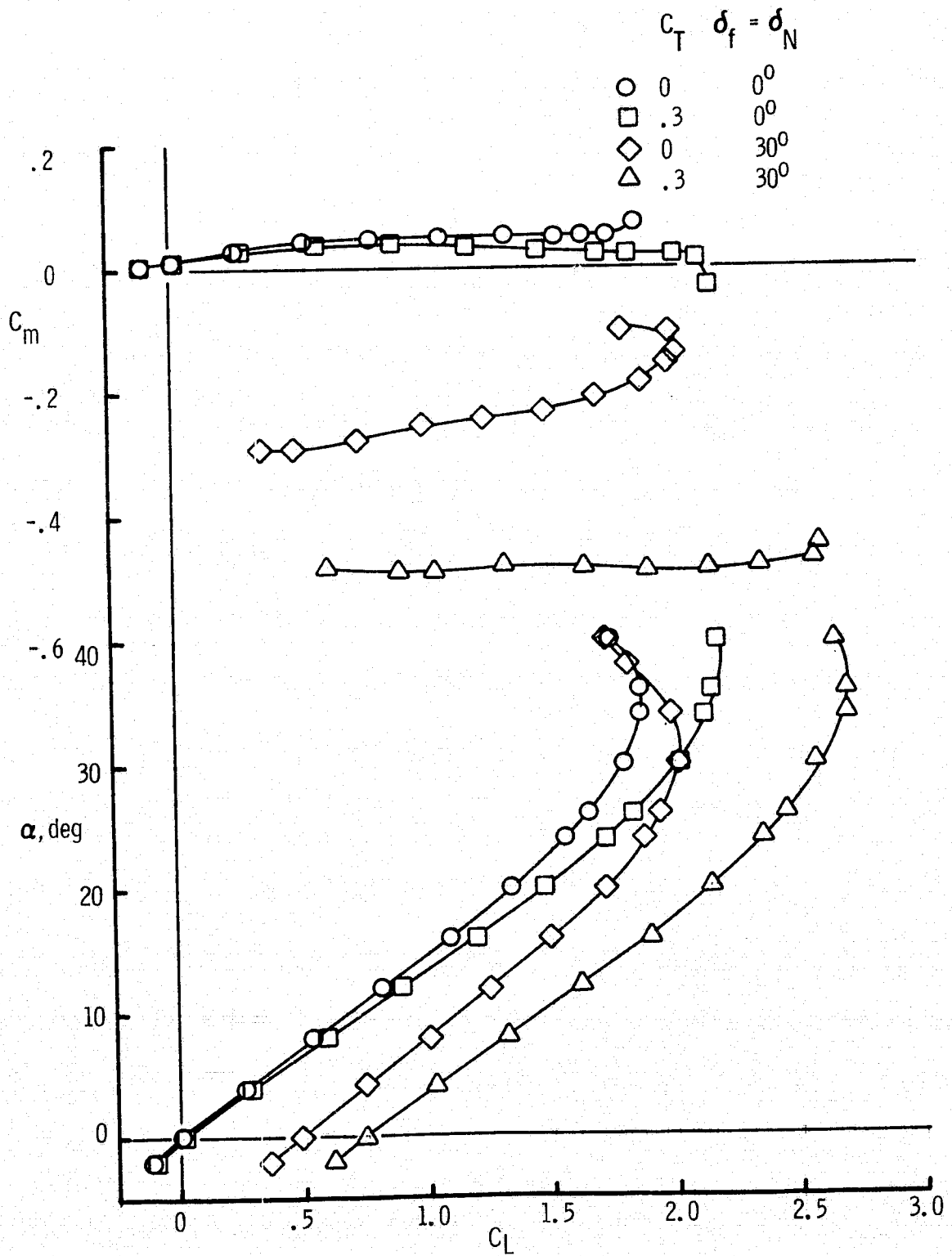


Figure 4. - Longitudinal characteristics of wing-canard configuration.

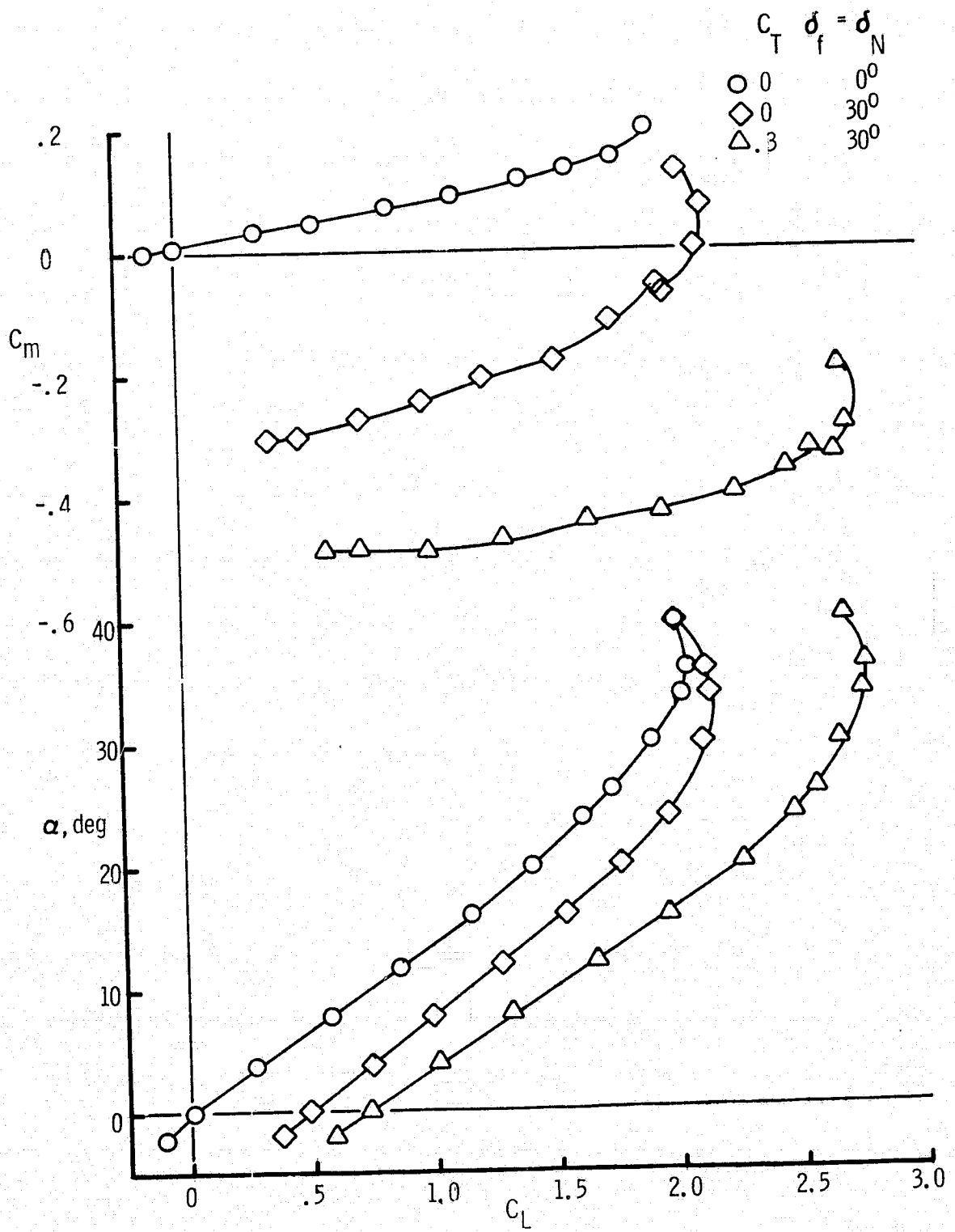


Figure 5. - Longitudinal characteristics of wing-canard-strake configuration.

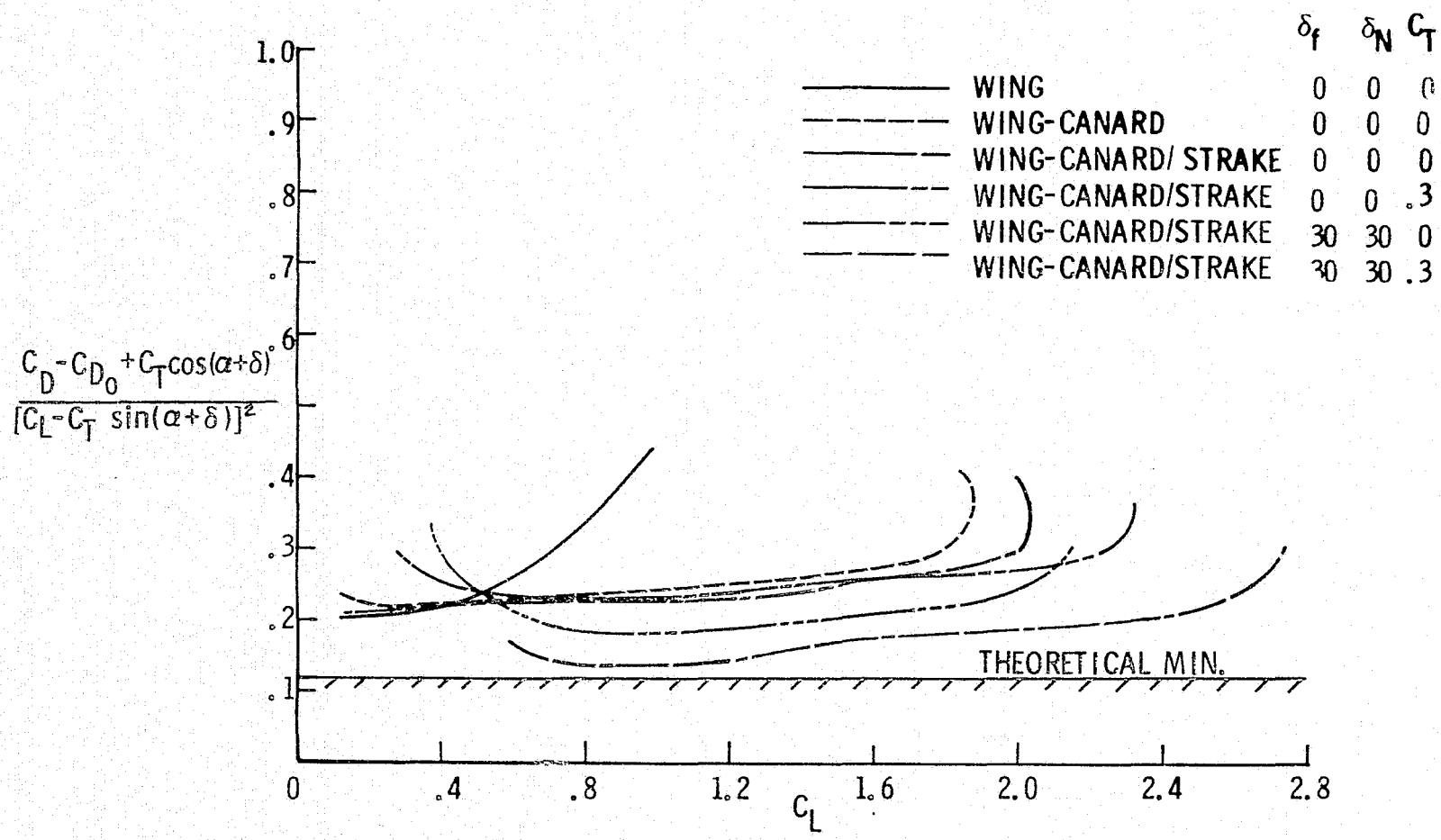


Figure 6. - Effect of configuration change on drag due to lift.

WING
AREA 0.45 m² (4.9 ft²)
SPAN 1.22 m (4.0 ft)
ASPECT RATIO 3.26
CANARD SPAN 0.83 m (2.72 ft)
NOZZLE ASPECT RATIO 4.0

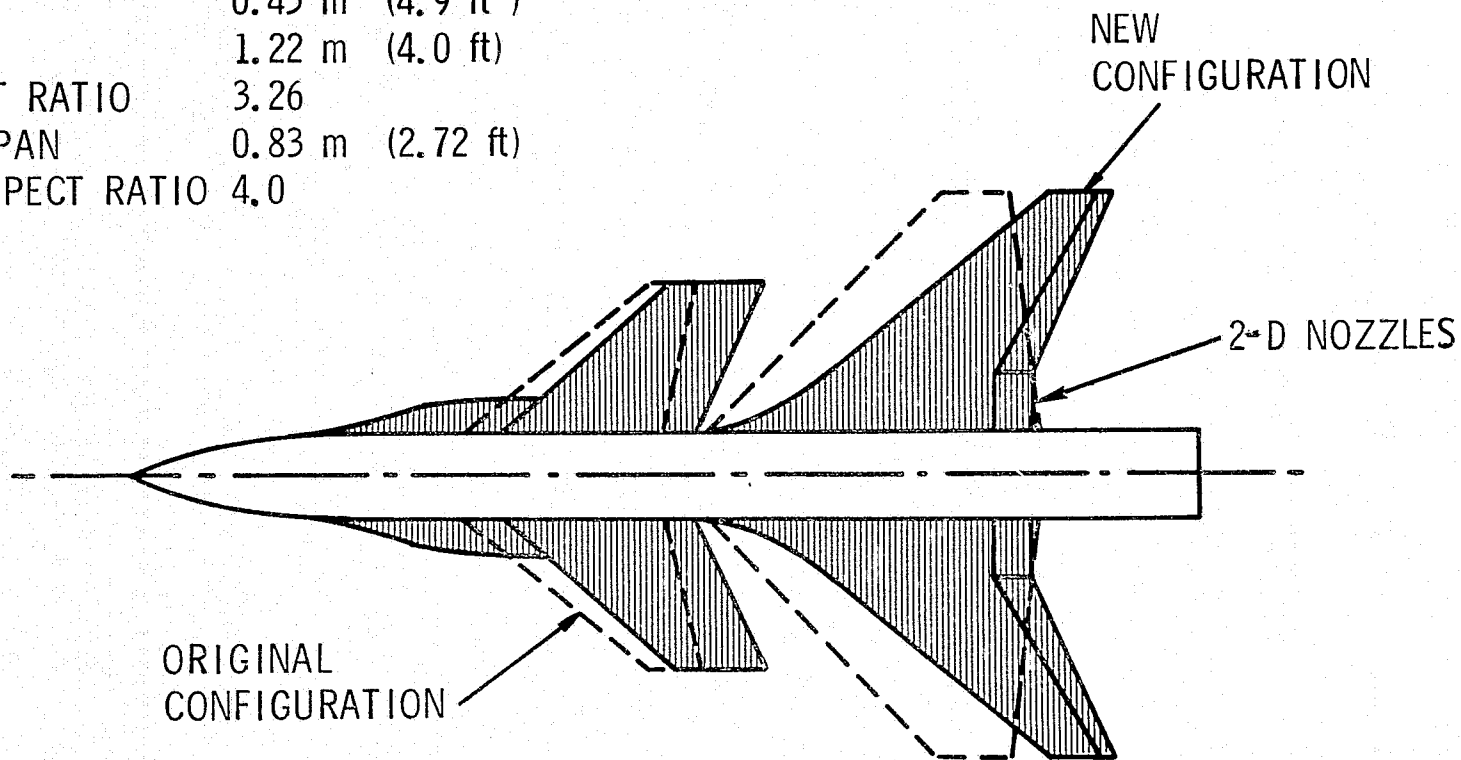


Figure 7. - New close-coupled wing-canard configuration.

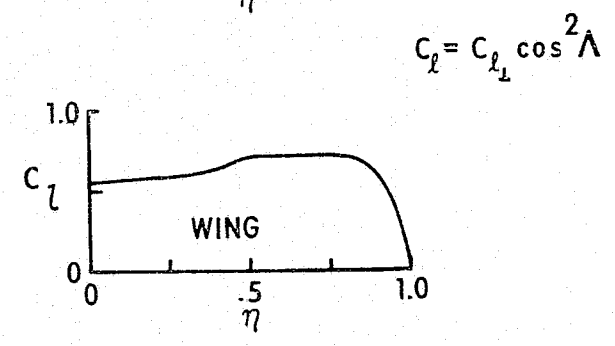
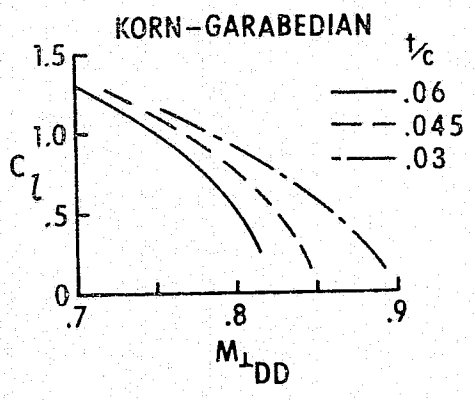
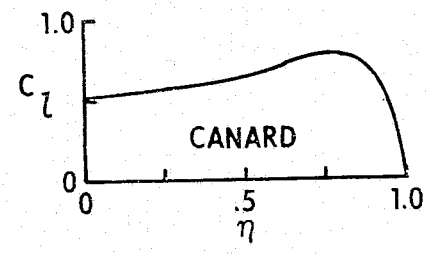
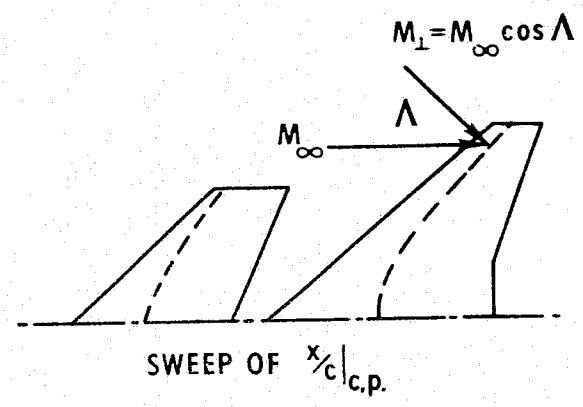
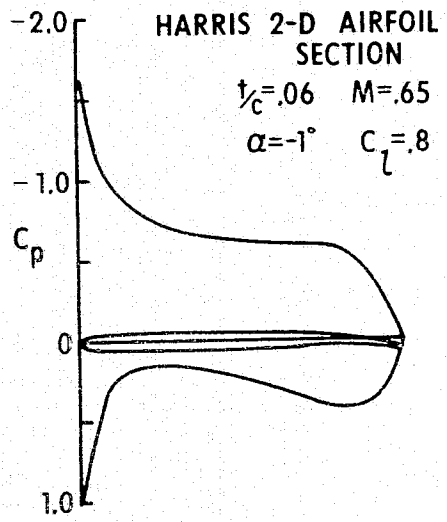


Figure 8. - Maximum section-lift coefficients based on drag divergence.

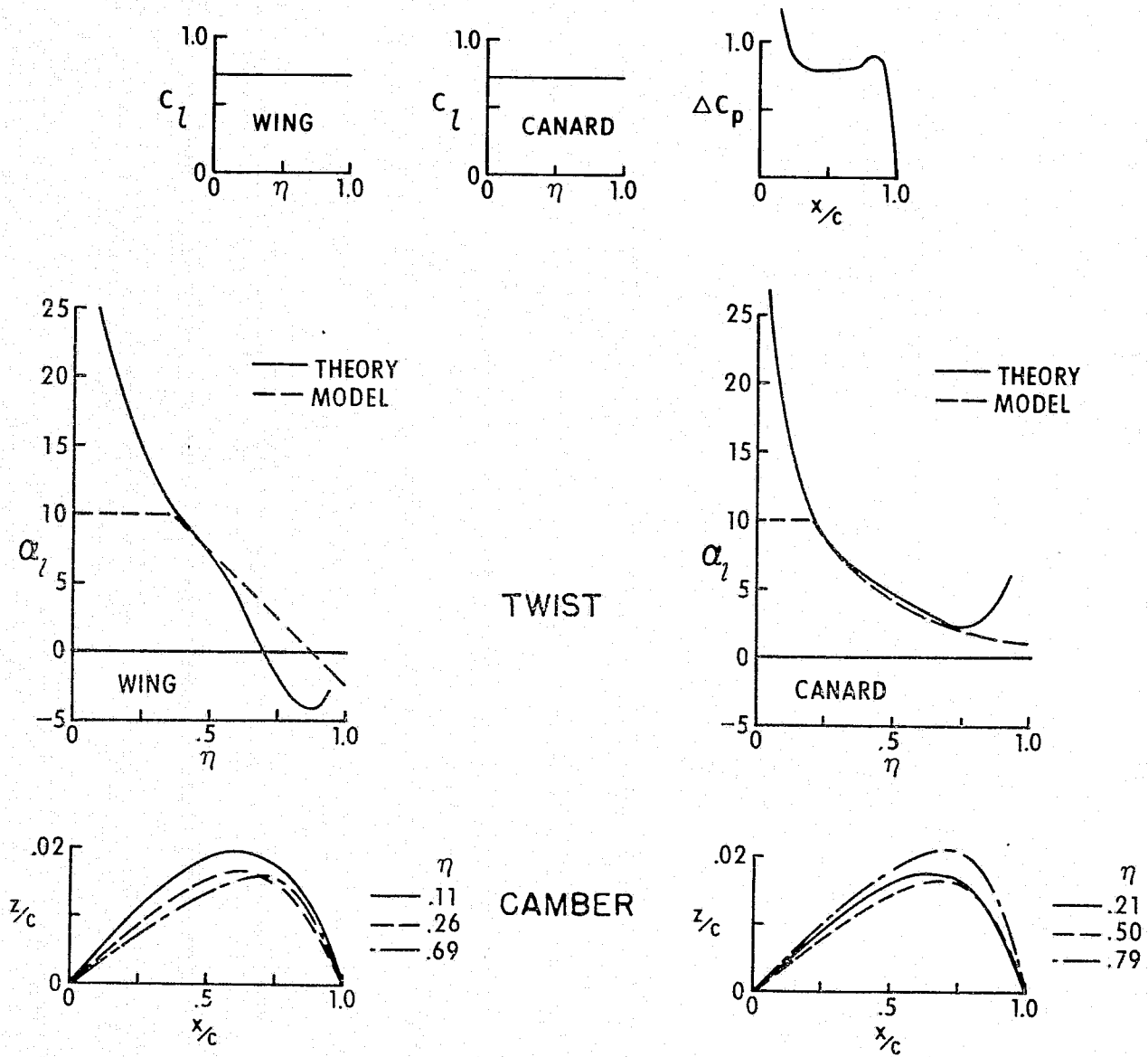


Figure 9. - Twists and cambers based on two-dimensional chord load and constant c_l .

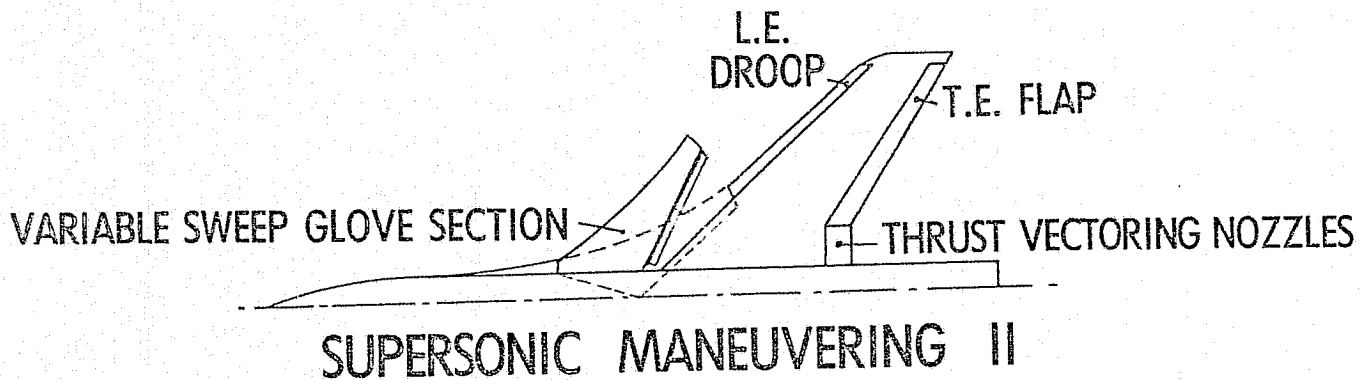
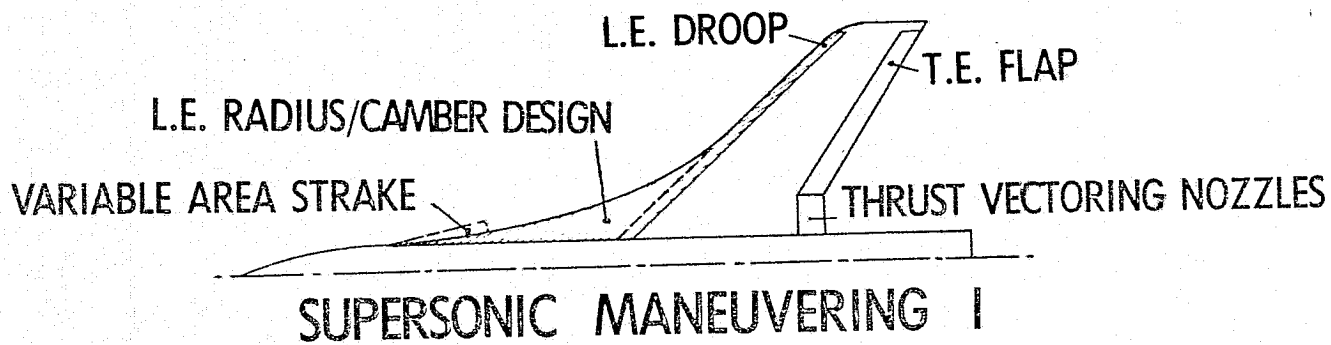


Figure 10. - Planned design of supersonic maneuver configuration.